Supporting information

Coordination ability determined transition metal ions substitution of Tb in Tb-Asp fluorescent nanocrystals and a facile ions detection approach

Jiazhi Duan[1#], Baojin Ma[1#], Feng Liu[1], Shan Zhang[1], Shicai Wang[1], Ying Kong[1], Min Du[1], Lin Han[3], Jianjun Wang[1], Yuanhua Sang[1*], and Hong Liu[1,2*]

[1]State Key Laboratory of Crystal Materials, Shandong University, Jinan, 250100, China

[2]Institute for Advanced Interdisciplinary Research (IAIR), University of Jinan, Jinan, 250022, China

[3]School of Microelectronics, Shandong University, Jinan, 250100, China

[*]Corresponding Author.
E-mail: Hong Liu, hongliu@sdu.edu.cn; Jianjun Wang, wangjianjun@sdu.edu.cn; Yuanhua Sang, sangyh@sdu.edu.cn; Lin Han, hanlin@sdu.edu.cn

[#]These authors contributed equally to this work and they should be regarded as co-first author.

S1 The ionic electronegativity χ of different ions.

Li^+	0.98	Mn^{2+}	1.55
Na^+	0.93	Fe^{2+}	1.83
K^+	0.82	Co^{2+}	1.88
Mg^{2+}	1.31	Ni^{2+}	1.91
Ca^{2+}	1.00	Cu^{2+}	2.0
Sr^{2+}	0.95	Zn^{2+}	1.65
Ba^{2+}	0.89		

Table. S1 The element electronegativity data (Pauling) from CHEMIX.

The ionic electronegativity χ of Li^+, Na^+, K^+, Mg^{2+}, Ca^{2+}, Sr^{2+} and Ba^{2+} were smaller than 1.4, and the ionic electronegativity χ of Mn^{2+}, Fe^{2+}, Co^{2+}, Ni^{2+}, Cu^{2+} and Zn^{2+} were bigger than 1.4. The different ionic electronegativity generated a different effect on the fluorescence intensity of Tb-Asp nanocrystals.

S2 The ionic electronegativity χ and valence V of different ions.

Ions	Fe^{2+}	Fe^{3+}	Cu^+	Cu^{2+}	Ag^+

electronegativity	1.83	1.9	1.9	2.0	1.93
valence	+2	+3	+1	+2	+1

Table. S2 The ionic electronegativity and valence of Fe^{2+}, Fe^{3+}, Cu^{+}, Cu^{2+} and Ag^{+}.

The ionic electronegativity of Fe^{2+}, Fe^{3+}, Cu^{+}, Cu^{2+}, Ag^{+} are similar, but the different ionic valence induced a different fluorescence decline.

S3 The ionic electronegativity χ and radius R of different ions.

Ions	Fe^{2+}	Hg^{2+}	Cu^{2+}	Pb^{2+}	Cu^{+}	Ag^{+}
electronegativity	1.83	2.0	2.0	2.33	1.9	1.93
radius	76	110	74	120	96	126

Table. S3 The electronegativity and radius of Fe^{2+}, Cu^{2+}, Hg^{2+}, Pb^{2+}, Cu^{+} and Ag^{+}.

The ionic electronegativity of Fe^{2+}, Cu^{2+}, Hg^{2+}, Pb^{2+}, Cu^{+} and Ag^{+} are similar, but the different ionic radius cause a different influence on the Tb-Asp fluorescence detection system.

S4 The morphology of Asp and Tb-Asp nanocrystals.

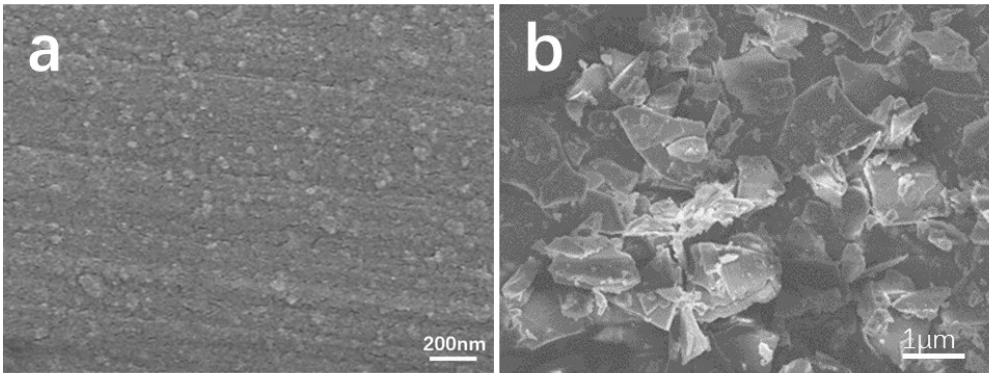

Fig. S1 (a) SEM image of Tb-Asp nanocrystals. (b) SEM image of original Asp.

As the SEM images show above, the Tb-Asp nanocrystals have an average size of 20 nm. However, the original Asp possesses uneven size distribution and disordered morphology. The size of some larger Asp can reach 20 μm, Compared the size difference, we can ascertain that the terbium nitrate has been reacted with Asp and formed uniform Tb-Asp nanocrystals.

S5 The excitation spectrum at 545 nm.

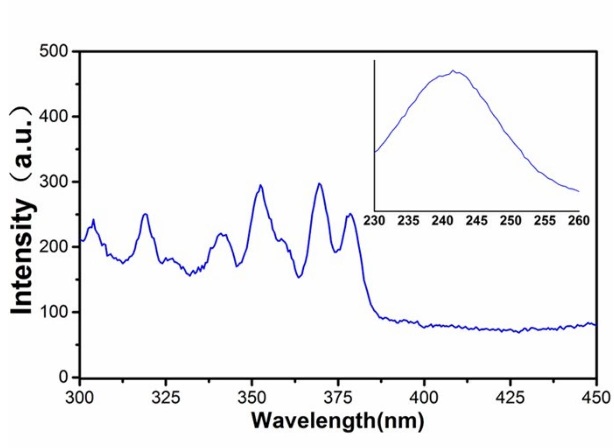

Fig. S2 The excitation spectrum 300-450nm (inset 230-260 nm) at 545 nm.

There are several absorption peaks in 300-450 nm and a broad strong absorption peak in 230-260 nm in the 545 nm excitation spectrum. The result indicates that the light in 230-260nm could effectively excite 545 nm light.

S6 The measurement of biocompatibility of Tb-Asp.

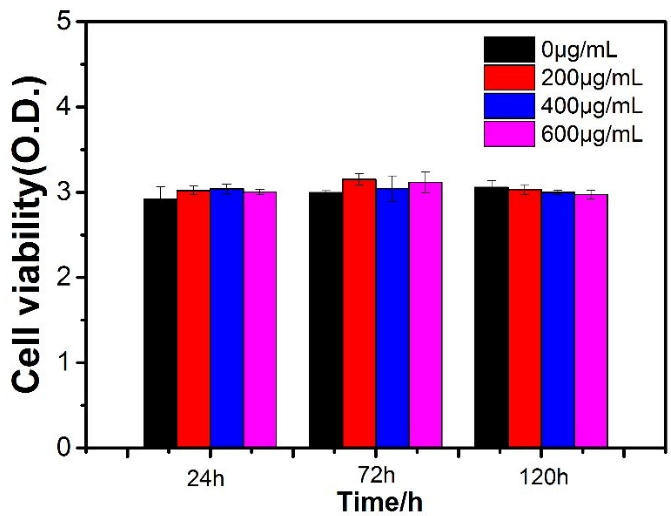

Fig. S3 The biocompatibility of Tb-Asp nanocrystals to Hela cells.

To confirm Tb-Asp nanocrystals possess high biocompatibility, Hela cells are chosen to measure the safety of Tb-Asp nanocrystals using Cell Counting Kit (CCK-8). As the Fig. S3 shows, the cell viability is very high, even when the concentration is up to 600 μg/mL, the cell viability still remain a high value. The high cell viability suggest that the Tb-Asp possesses a good biocompatibility.

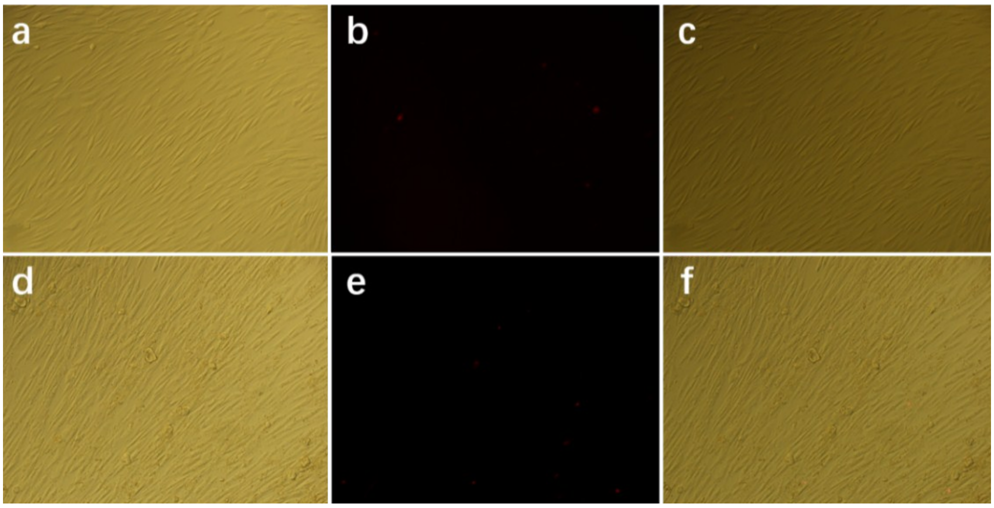

Fig. S4 PI staining at 0 μg/mL, 600 μg/mL Tb-Asp nanocrystals concentration respectively. (a), (d) under bright field; (b), (e), at 543 nm excitation; (c), (f) merge of bright field and 543 nm excitation.

Propidium iodide (PI) which can only mark the dead cell staining (Fig. S4) was performed at 0 μg/mL, 600 μg/mL Tb-Asp concentration respectively. On the both two condition, there are only a little dead cells. Therefore, it is obvious that Tb-Asp nanocrystals is of high security.

S7 Photograph of Tb-Asp and Cu-Asp under the condition of visible light and 250nm light.

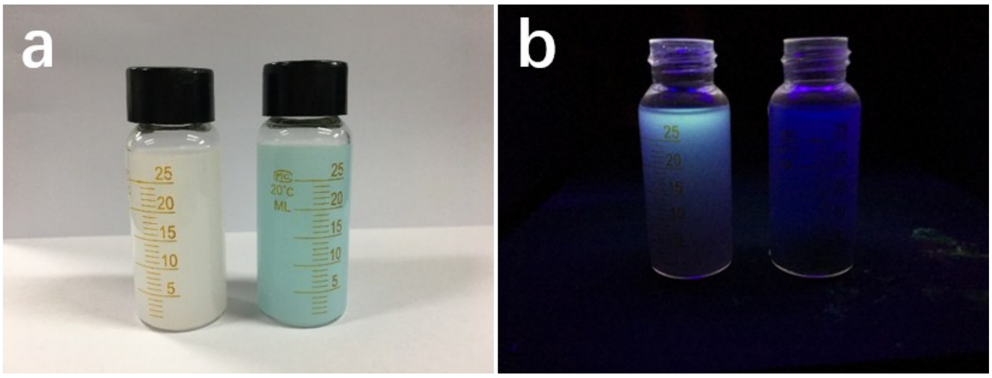

Fig. S5 Tb-Asp and Cu/Tb-Asp suspension. (a) Tb-Asp (left) and Cu/Tb-Asp (right) under sunlight. (b) Tb-Asp (left) and Cu/Tb-Asp (right) under 250nm light.

The liquid in the left bottle in both photo is Tb-Asp solution and the right is the Cu/Tb-Asp solution after the substitution of copper ions to Tb-Asp solution, the concentration of the two solutions is 40 mg/mL. (a) is the photo under the condition of visible light and (b) is excited by 250 nm UV light. As the contrast of (a) and (b) vividly shows, after the addition of copper ions, the Tb-Asp solution changed its color and lost its fluorescence. The result corresponds well with the copper ions detection experiment.

S8 The EPMA quantitative Result of Cu/Tb-Asp.

Element	Mass %	Mol %
Cu	1.21	2.97
Tb	98.79	97.03
Total	100	100

Table. S4 The mass ratio and mole ratio between Cu and Tb content.
Corr Method : ZAF4. Coating Element : C

To figure out the ratio of Cu and Tb in the Cu/Tb-Asp nanocrystals, the EPMA quantitative analysis were carried out. As shown in Table. S4, the EPMA quantitative result demonstrate that the mass ratio and mole ratio of Cu relative to Tb in Cu/Tb-Asp are 1.21% and 2.97% respectively, the mass ratio and mole ratio of Tb relative to Cu in Cu/Tb-Asp are 98.79% and 97.03% respectively. The result suggests that only a small amount of copper ions react with Tb-Asp nanocrystals and cause the fluorescence quenching of Tb-Asp nanocrystals.

S9 Tb3d and Cu2p scan spectra.

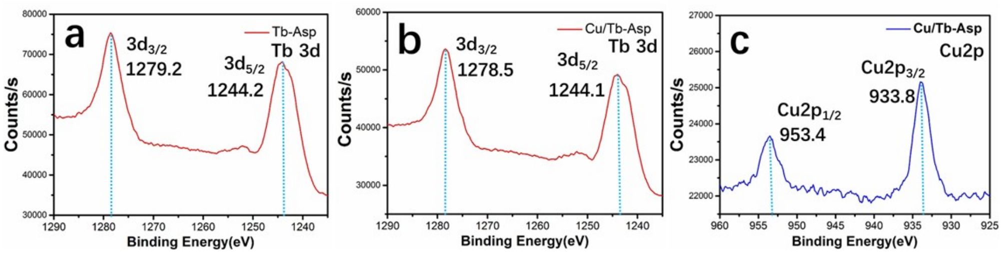

Fig. S6 The Tb3d and Cu2p scan spectra. (a) The Tb3d scan spectra of Tb-Asp nanocrystals. (b) The Tb3d scan spectra of Cu/Tb-Asp. (c) The Cu2p scan spectra of Cu/Tb-Asp.

As is shown in Fig. S6 (a) and (b), the peaks in Tb3d scan spectra are in a similar location, more concretely, the binding energy of $Tb3d_{3/2}$ and $Tb3d_{5/2}$ are consistent with previous report and almost the same, which shows that the Tb element in both Tb-Asp and Cu/Tb-Asp nanocrystals possess the same property. The Cu2p scan spectra shows that the $Cu2p_{3/2}$ binding energy is 933.8eV, and $Cu2p_{1/2}$ binding energy is 953.4eV, which proves that the valence of copper ions in Cu/Tb-Asp nanocrystals is +2. The scan result indicates that the Cu element exist in the Cu/Tb-Asp nanocrystals, which fully prove that the copper ions reacted with Tb-Asp nanocrystals.

S10 1H solid state NMR

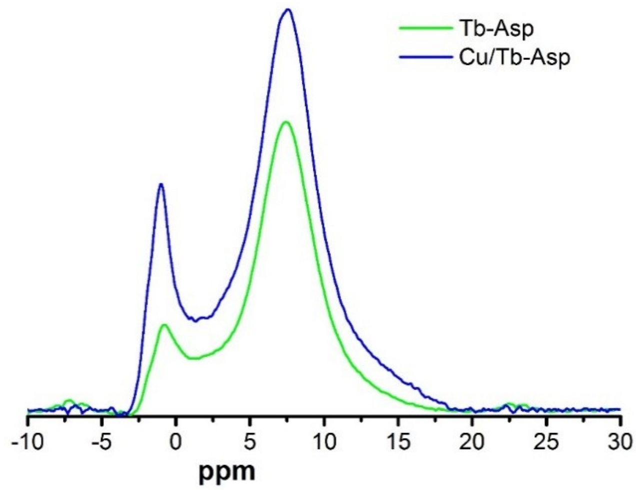

Fig. S7 The 1H solid state NMR of Tb-Asp and Cu/Tb-Asp.

As is show in Fig. S7, the ^{1}H solid state NMR result shows that the peaks of Tb-Asp and Cu/Tb-Asp are almost the same. However, the peak location of Cu/Tb-Asp is 7.545 ppm and the peak of Tb-Asp locates at 7.422 ppm. The result reveals that the Cu ions substitute Tb ions and thus induces a similar peak information but a higher chemical shift.

S11 UV-Vis light absorption spectrum

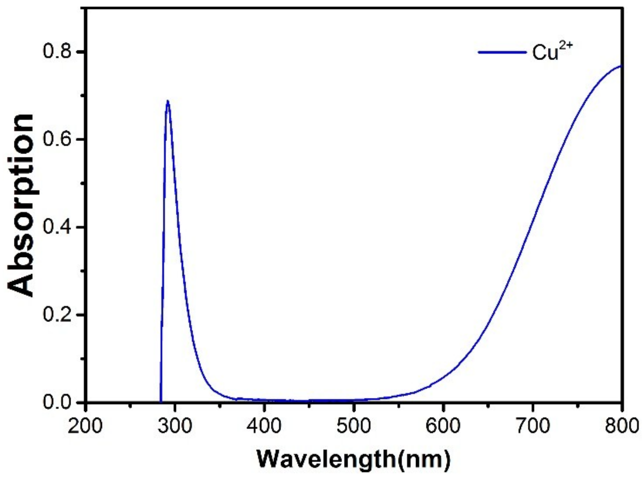

Fig. S8 The UV-Vis light absorption spectrum of Cu^{2+}.

From the UV-Visual absorption spectrum result, it is clear the Cu^{2+} has no absorption in 250 nm and little absorption in 545 nm. This result suggests that the fluorescence quenching is not caused by the light absorption of Cu^{2+} when Tb-Asp nanocrystals are excited by 250 nm light.

S12 UV-Vis light absorption spectrum

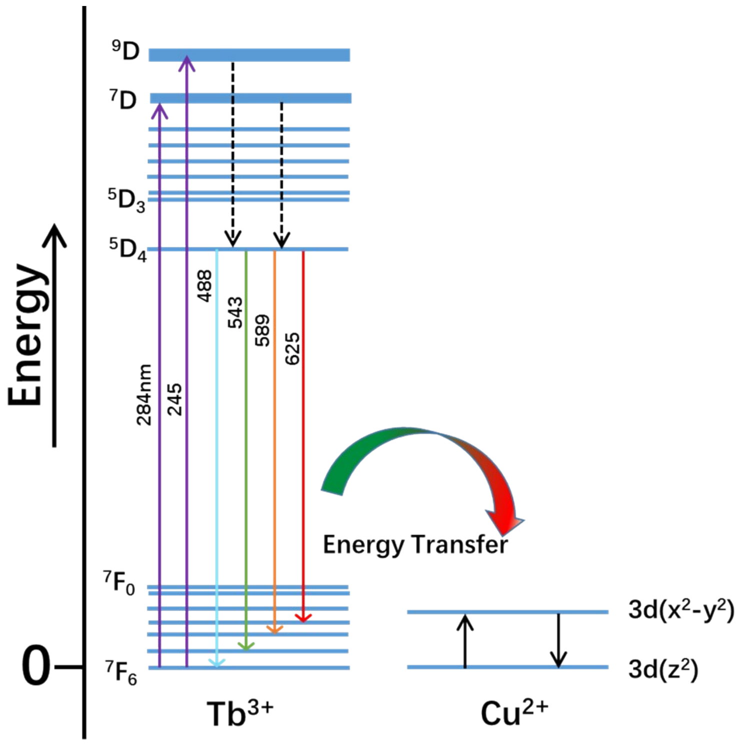

Fig. S9 The energy level diagram and proposed energy-transfer mechanisms for fluorescence quenching.